A&A 472, L43–L46 (2007)
DOI: 10.1051/0004-6361:20078165

Astronomy & Astrophysics

Letter to the Editor

A revision of the solar manganese abundance using new and remeasured laboratory oscillator strengths⋆,⋆⋆

R. Blackwell-Whitehead[1] and M. Bergemann[2]

[1] Blackett Laboratory, Imperial College London, London SW7 2AZ, UK
e-mail: r.blackwell@imperial.ac.uk
[2] Institute for Astronomy and Astrophysics, Ludwig-Maximilian University, Scheinerstr. 1, 81679 Munich, Germany
e-mail: mbergema@usm.uni-muenchen.de

Received 26 June 2007 / Accepted 10 July 2007

ABSTRACT

Context. The solar photospheric element abundances are generally in good agreement with the meteoritic CI chondrite abundances, with the exception of a small number of elements including manganese. The solar photospheric abundances, determined using model atmospheres, include laboratory oscillator strengths where available. However, the current laboratory database for Mn I oscillator strengths is derived from several different laboratory observations determined from several different laboratory techniques. The uncertainty in the solar photospheric manganese abundance and the difference between it and the meteoritic CI chondrite abundance may just be an artefact of inaccurate laboratory data.
Aims. The aim of our new laboratory measurements is to measure a self consistent set of accurate absolute oscillator strengths and use the new laboratory data to re-evaluate the solar manganese abundance.
Methods. New and more accurate oscillator strengths have been determined by combining branching fractions with previously measured energy level lifetimes. Using the new laboratory data, the solar photospheric abundance of manganese has been determined with theoretical and semi-empirical model atmospheres, MAFAGS-ODF and Holweger & Müller, respectively.
Results. We present experimental oscillator strengths for 94 Mn I transitions covering the wavelength range 2384 to 17 744 Å. Using 22 relatively un-blended solar Mn I transitions, we determine the photospheric abundance of manganese to be $\log \varepsilon_{\odot} = 5.37 \pm 0.05$ dex.
Conclusions. The new value is in good agreement with previous photospheric abundance determinations. The implications for the solar photospheric and meteoritic CI chondrite abundance is discussed.

Key words. atomic data – line: identification – methods: laboratory – Sun: abundances

1. Introduction

The chemical abundance of the solar photosphere is generally accepted to be in good agreement with the CI chondrite meteors to within the uncertainty of the currently accepted elemental abundance values. However, for several elements (e.g. Ga, Mn, In, Sn, Tm, Yb, Hf, see Lodders 2003) there is a significant difference between the solar photospheric and the meteoritic CI chondrite abundance. In particular, there is a large disagreement between the reference abundance of manganese in the solar photosphere (5.39 ± 0.03 dex) and in the CI chondrites (5.50 ± 0.03), see Lodders (2003) and references therein. This discrepancy is thought to be due to several factors including: uncertainties in the damping and hyperfine structure parameters, the assumption that line formation is in LTE, and unknown blends. Recently, Bergemann & Gehren (2007, hereafter Paper I) reanalysed the photospheric Mn abundance to $\log \varepsilon_{\odot} = 5.36 \pm 0.1$ dex, taking account of these methodical inaccuracies, but the reason for the discrepancy still remained elusive. In this paper we re-evaluate the solar abundance of manganese using the new and remeasured transition probabilities for 22 Mn I lines, with uncertainties of ≤ 0.05 dex. We perform NLTE statistical equilibrium calculations and spectrum synthesis for the semi-empirical Holweger & Müller model atmosphere (Holweger & Müller 1974) and for the theoretical line-blanketed LTE model atmosphere MAFAGS-ODF (see a review in Grupp 2004). As is the case with all other line-blanketed atmospheric models of this type so far, we have not attempted to model the solar chromosphere. Furthermore, the influence of van der Waals damping on the line profiles is also investigated.

2. Laboratory oscillator strengths

The accuracy of the current laboratory database for Mn I oscillator strengths varies considerably with wavelength and source publication. The large photospheric – meteoritic difference may be due to unaccounted uncertainties in the photospheric calculations introduced by the different techniques used to determine oscillator strengths in previous laboratory measurements. Blackwell & Collins (1972) and Booth et al. (1984a) both used absorption techniques to determine oscillator strengths. In particular, Booth et al. (1984a) quotes uncertainties as low as 3 per cent, but Booth's uncertainties have been been independently moderated in the NIST (National Institute of Standards and Technology, USA) atomic spectra database to be of the order of 10 to 20 per cent, see Fuhr & Wiese (2003). Greenlee & Whaling (1979) used emission spectroscopy to determine

⋆ Research supported by the International Max Planck Research School(IMPRS), Munich, Germany.
⋆⋆ Full Table 1 is only available at http://www.aanda.org

oscillator strengths, and their measurements include many of the transitions relevant to our current study of the solar photosphere, but the uncertainty in their oscillator strengths is of the order 25 per cent. Furthermore, there are several strong ($\log gf > -1.00$) relatively un-blended visible solar Mn I lines that have no laboratory determined oscillator strengths. A full discussion of the status of the published literature on laboratory oscillator strengths for Mn I can be found in Blackwell-Whitehead et al. (2005b).

The new and remeasured laboratory oscillator strengths have been determined by combining branching fractions with level lifetimes. The branching fractions are determined from high resolution, intensity calibrated spectra for manganese measured at Imperial College using Fourier transform spectroscopy. The spectra are intensity calibrated using two intensity standard lamps calibrated at the National Physical Laboratory, Teddington. Both lamps have a minimum two standard deviation uncertainty of 3 per cent. The Mn I wavenumbers in Table 1 have been calibrated using 20 Ar II transitions from Norlén (1973) and the wavenumber calibration uncertainty is 0.005 cm^{-1}, which corresponds to an uncertainty of 0.0008 Å at 4000 Å. Further details of the experimental conditions, intensity and wavelength calibration for the manganese spectra are given in Blackwell-Whitehead et al. (2005b). The level lifetimes are taken from Schnabel et al. (1995) for all upper levels where available with the exception of the $e^6S_{2.5}$ level which is taken from the earlier work of Marek (1975).

The uncertainty in the branching fractions in column five of Table 1 are determined from the individual uncertainty for each transition and the uncertainty when transferring the intensity calibration between separate spectra. The uncertainty in the oscillator strengths presented in Table 1 is the sum in quadrature of the uncertainty in the branching fractions and the level lifetimes.

The majority of the strong transitions ($\log gf > -1.00$) measured by Greenlee & Whaling (1979) agree with our laboratory oscillator strengths to within the combined uncertainty of the two sets of values, see Fig. 1, but it should be noted that our uncertainties are much lower than those of Greenlee & Whaling (1979). In addition, over half of the oscillator strengths published by Booth et al. (1984a) agree with our values to within the combined uncertainties. However, for several strong transitions there is a considerable difference between our results and those of Booth et al. (1984a). In particular, Booth et al. (1984a) indicates that the 6013.489 and 6021.793 Å transitions from the $e^6S_{2.5}$ level are twice as strong as our measurements. Indeed, Kurucz & Bell (1995) use the $\log gf$ values of Booth et al. (1984a) for the $e^6S_{2.5}$ transitions. However, when we compare our new laboratory measurements for the previously unmeasured $e^6S_{2.5}$ branches with the calculations of Kurucz & Bell (1995) we observe a much closer agreement. The disagreement between the red and near infrared $\log gf$ values for Mn I has been discussed by Blackwell-Whitehead et al. (2005b) and a general deviation in the absolute scale of the Oxford oscillator strengths in the infrared has been noted and discussed in Blackwell-Whitehead et al. (2006).

3. NLTE calculations and spectrum synthesis

The statistical equilibrium calculations were performed for the Holweger-Müller (HM) and MAFAGS-ODF (ODF) model atmospheres. The manganese model atom and method are essentially the same as in Paper I. The total number of levels for the three ionization stages was 459 and the total number of lines 2809. Wavelengths and oscillator strengths were all taken from the Kurucz database (Kurucz & Bell 1995). The only difference in the atomic model, when compared to our model in Paper I, is that the photoionization cross-sections are now computed from Kramers' formula with the *effective* quantum numbers for all levels. This correction was introduced due to the complexity of the atom, i.e., existence of numerous doubly excited configurations, which, opposite to those of single excitation, can not be simultaneously treated in a simple hydrogenic approximation. The hydrogen collision rates were computed according to Drawin's formula, see Steenbock & Holweger (1984). A full discussion of the interaction processes leading to NLTE equilibria in Mn I based on the MAFAGS-ODF model atmosphere can be found in Paper I.

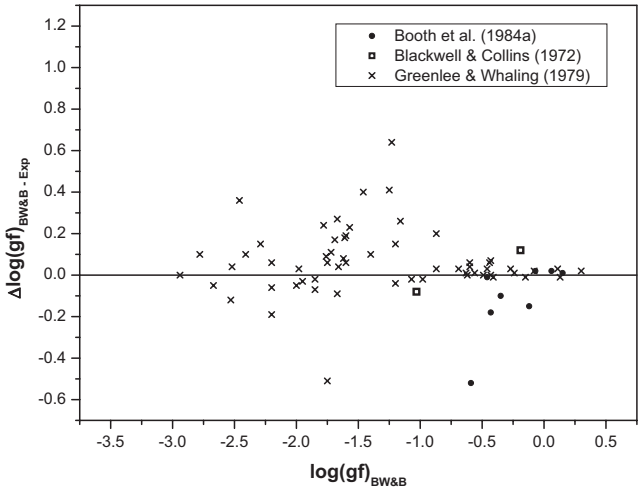

Fig. 1. A comparison of previous laboratory determined oscillator strengths with our new and remeasured values.

The NLTE departure coefficients were used to generate profiles of Mn I lines with the spectrum synthesis code SIU. For all other elements LTE is assumed. The solar spectrum is calculated using the HM and ODF model atmospheres, with a Mn abundance of $\log \varepsilon_\odot = 5.47$ dex and a constant microturbulence velocity of $\xi_t = 0.9$ km s^{-1}. The computed spectrum is compared with the observed spectrum from the Kitt Peak Solar Flux Atlas (Kurucz et al. 1984). The line broadening parameters were set at a rotational velocity of $V_{\rm rot} = 1.8$ km s^{-1} and a macroturbulence velocity of $V_{\rm mac} = 2.5 \ldots 4$ km s^{-1}. Van der Waals damping constants C_6 are computed according to Anstee & O'Mara (1995); initially only a correction of $\Delta \log C_6 \approx -0.1$ is applied in order to fit the wings of strong lines. All parameters for the lines are given in Table 2 with the exception of the hyperfine structure data which is given in Paper I.

4. Solar abundance of Mn

The NLTE results for both the HM and ODF model atmospheres are presented in Table 2. We obtain the average weighted[1] NLTE abundance of 5.35 ± 0.08 dex for the ODF model atmosphere and 5.46 ± 0.08 dex for the HM model atmosphere, where the uncertainty is one standard deviation. The LTE abundances, derived with the ODF and HM models are 5.33 ± 0.1 dex and 5.49 ± 0.08 dex, respectively. The systematic difference in NLTE abundances, $\Delta \log \varepsilon$(HM − ODF) = 0.11, reflects the different

[1] The abundances were weighted according to the uncertainties in the oscillator strength measurements.

Table 1. New and remeasured laboratory oscillator strengths for Mn I, the complete table is available online.

Upper level	Lower level	Wavenumber (cm^{-1})	λ_{air} (Å)	*BF*	This Work Log (gf)	This Work *Unc.* (dex)	Previous Work Log (gf)	Previous Work Ref.[b]	Calc.[a] Log (gf)
$e\ ^6S_{2.5}$	$z\ ^8P_{3.5}$	22 872.341	4370.8646	0.0003	–3.59	0.08			–3.03
E = 41 403.93 cm^{-1}	$z\ ^6P_{1.5}$	16 624.678	6013.4885	0.2134	–0.43	0.05	–0.25	3	–0.25
τ = 18.5 ± 1.8 ns[c]	$z\ ^6P_{2.5}$	16 615.976	6016.6380	0.3211	–0.25	0.05			–0.22
	$z\ ^6P_{3.5}$	16 601.751	6021.7932	0.4280	–0.12	0.05	0.03	3	0.03
	$y\ ^6P_{1.5}$	5714.003	17 496.0867	0.0089	–0.88	0.05			–0.93
	$y\ ^6P_{2.5}$	5678.129	17 606.6275	0.0123	–0.73	0.05			–0.77
	$y\ ^6P_{3.5}$	5634.016	17 744.4833	0.0156	–0.62	0.05			–0.67
Residual				0.0005					

[a] The semi-empirical calculations are taken from Kurucz & Bell (1995).
[b] The previous laboratory values are taken from (1) Greenlee & Whaling (1979); (2) Blackwell & Collins (1972); and (3) Booth et al. (1984a).
[c] Lifetime for the level e $^6S_{2.5}$ is taken from Marek (1975).

Table 2. Lines selected for solar abundance calculation. The NLTE abundances refer to MAFAGS-ODF (ODF) and Holweger & Müller (HM) model atmospheres. Van der Waals damping interaction constants $\log C_6$ are computed according to Anstee & O'Mara (1995); a correction of $\Delta \log C_6 \approx -0.1$ is applied in order to fit the wings of strong lines.

No.	λ [Å]	Mult.	N_{HFS}	E_{low} [eV]	Lower level	Upper level	W_λ [mÅ]	$\log gf$	Error	$\log C_6$	$\log \varepsilon_\odot$ ODF	$\log \varepsilon_\odot$ HM
1	4055.513	5	4	2.13	$a\ ^6D_{3.5}$	$z\ ^6D^o_{3.5}$	136.	–0.08	0.03	–31.0	5.34	5.48
2	4070.264	5	3	2.19	$a\ ^6D_{0.5}$	$z\ ^6D^o_{0.5}$	70.	–1.03	0.02	–31.0	5.50	5.66
3	4436.342	22	3	2.91	$a\ ^4D_{2.5}$	$z\ ^4D^o_{1.5}$	71.3	–0.43	0.02	–30.65	5.40	5.53
4	4451.581	22	3	2.88	$a\ ^4D_{3.5}$	$z\ ^4D^o_{3.5}$	93.	0.13	0.02	–30.75	5.27	5.40
5	4453.001	22	2	2.93	$a\ ^4D_{1.5}$	$z\ ^4D^o_{0.5}$	53.5	–0.62	0.02	–30.6	5.45	5.56
6	4498.901	22	2	2.93	$a\ ^4D_{1.5}$	$z\ ^4D^o_{2.5}$	57.	–0.46	0.02	–30.7	5.44	5.56
7	4502.220	22	2	2.91	$a\ ^4D_{2.5}$	$z\ ^4D^o_{3.5}$	59.	–0.43	0.02	–30.7	5.26	5.37
8	4671.667	21	5	2.88	$a\ ^4D_{3.5}$	$z\ ^4F^o_{2.5}$	12.8	–1.66	0.02	–30.73	5.33	5.47
9	4709.705	21	4	2.88	$a\ ^4D_{3.5}$	$z\ ^4F^o_{3.5}$	72.	–0.49	0.02	–30.74	5.28	5.40
10	4739.088	21	4	2.93	$a\ ^4D_{1.5}$	$z\ ^4F^o_{1.5}$	62.	–0.60	0.02	–30.71	5.35	5.46
11	4754.021	16	5	2.27	$z\ ^8P^o_{2.5}$	$e\ ^8S_{3.5}$	146.	–0.07	0.02	–30.7	5.29	5.43
12	4761.508	21	4	2.94	$a\ ^4D_{0.5}$	$z\ ^4F^o_{1.5}$	73.	–0.27	0.02	–30.75	5.39	5.49
13	4762.358	21	5	2.88	$a\ ^4D_{3.5}$	$z\ ^4F^o_{4.5}$	108.	0.30	0.02	–30.86	5.23	5.34
14	4765.851	21	3	2.93	$a\ ^4D_{1.5}$	$z\ ^4F^o_{2.5}$	81.	–0.08	0.02	–30.86	5.30	5.40
15	4766.413	21	4	2.91	$a\ ^4D_{2.5}$	$z\ ^4F^o_{3.5}$	98.5	0.11	0.02	–30.84	5.26	5.37
16	4783.389	16	5	2.29	$z\ ^8P^o_{3.5}$	$e\ ^8S_{3.5}$	148.	0.06	0.02	–30.7	5.27	5.37
17	4823.460	16	6	2.31	$z\ ^8P^o_{4.5}$	$e\ ^8S_{3.5}$	149.	0.15	0.02	–30.7	5.26	5.39
18	5117.913	32	3	3.12	$a\ ^4G_{2.5}$	$z\ ^4F^o_{1.5}$	24.2	–1.20	0.02	–30.61	5.49	5.58
19	5255.287	32	6	3.12	$a\ ^4G_{5.5}$	$z\ ^4F^o_{4.5}$	41.5	–0.87	0.04	–30.76	5.39	5.48
20	6013.465	27	6	3.06	$z\ ^6P^o_{1.5}$	$e\ ^6S_{2.5}$	87.	–0.43	0.05	–30.64	5.37	5.46
21	6016.586	27	6	3.06	$z\ ^6P^o_{2.5}$	$e\ ^6S_{2.5}$	97.8	–0.25	0.05	–30.64	5.37	5.46
22	6021.727	27	6	3.06	$z\ ^6P^o_{3.5}$	$e\ ^6S_{2.5}$	96.8	–0.12	0.05	–30.64	5.35	5.45

temperature structure of the models. The HM model is approximately 100 ∼ 150 K hotter than the ODF model at $\log \tau_{5000}$ above –0.5. The line-to-line scatter is of the same magnitude in both atmospheric models. The influence of photoionization on the line profiles is not uniform: an increase in cross-sections by a factor of 300 (as expected for Mn atom) yields the corrections to different lines in the range from –0.09 to +0.02 dex. A certain amount of the remaining discrepancies can be explained by uncertainties in the van der Waals damping constants. A correction of $\Delta \log C_6 \approx -0.4$ relative to Anstee & O'Mara values was applied to the lines of all multiplets. However, only strong lines were indeed sensitive to this procedure. We note that to a certain degree C_6 and abundance can be exchanged in their influence on line profiles, hence this correction remains just a free parameter. However, this procedure yields a smaller rms abundance scatter $\log \varepsilon_\odot = 5.37 \pm 0.05$ dex, which we accept as our *new revised solar abundance of Mn*. The NLTE value of $\log \varepsilon_\odot = 5.37 \pm 0.01$ dex for the MAFAGS-ODF model is also obtained from three lines of multiplet 27 (6013.465, 6016.586 and 6021.727 Å), which are the most commonly used lines for Mn abundance analyses of the Sun and other stars. This result is consistent with our previously suggested solar NLTE Mn abundance of 5.36 ± 0.1 dex (Paper I), determined from 12 lines with low uncertainties in the laboratory determined $\log gf$ values. However, the new oscillator strengths used in this paper lead to a smaller fitted-abundance spread between lines of different multiplets and provide a larger number of self consistent absolute oscillator strengths which reduces the uncertainty from unidentified blends.

5. Discussion

Our results indicate that the remaining ∼0.13 dex difference between meteoritic CI chondrite and the solar photospheric

abundance determined from the MAFAGS-ODF model with NLTE assumption are, most likely, due to the "missing atomic data" problem. In comparison, the Holweger & Müller model atmosphere delivers LTE and NLTE abundances that are in a good agreement with the meteoritic value within their combined uncertainties.

At this stage of refinement the solar Mn abundance, in the absence of the proper atomic data, depends on the choice of the atmospheric model. What model should be given a preference, rests solely on the purposes of the reader. If one wants to obtain the abundance, absolutely consistent with the meteoritic, he may use the HM model and LTE. This result is not new and was repeatedly confirmed by other authors (see discussion in Rutten 2002). However, we refrain from this approach based on the following grounds:

- The HM LTE and ODF NLTE average abundances have equal standard deviations 0.08 dex. This is the evidence that some common parameters, used in spectrum synthesis, are erroneous (assumption of constant microturbulence, damping and/or oscillator strengths). As shown by Gehren et al. (2001), the rms scatter of abundances obtained with a single set of oscillator strengths is a measure of the accuracy of the mean solar Fe I abundance that can be reached with these $\log gf$ data. Our results for Mn I indirectly confirm their deduction. For instance, the solar Mn I line at 5004 Å produces an incredibly small abundance of 4.9 dex, hence it was ignored for the abundance analysis. This line is weak and almost unblended that casts doubt on its $\log gf$ value.
- The temperature structure of the HM model was calculated using the LTE assumption for formation of solar iron lines. Hence, any LTE abundance analysis with this model will produce internally self-consistent results. However, they will not neccessarily be consistent with the real atmosphere, which is far from LTE.
- Strong Mn I lines are not reproduced in LTE with both atmospheric models due to different line shapes: too shallow cores and broad middle wings. Their abundances can not be reliably estimated.

If the principal goal of a reader is to perform differential analysis of other stars with respect to the Sun, then results of NLTE calculations with ODF atmospheric model (5.37 ± 0.05 dex) should be used. We emphasize that a *reduction of rms abundance scatter by 0.05* dex, when compared to our solar Mn abundance from Paper I (5.36 ± 0.1 dex), is due to the new oscillator strengths, adjustment of damping constants and adoption of effective quantum numbers in calculation of photoionization cross-sections with Kramer's formula. In this case, the discrepancy of 0.13 dex with the meteoritic value may be partly eliminated by use of appropriate photoionization cross-sections. We suggest that manganese, similar to the comparable atoms (Fe, Si) for which quantum-mechanical calculations are available (see Grupp 2004, Fig. 5), requires few orders of magnitude larger cross-sections than the hydrogenic approximation. In addition, stronger lines produce a Mn underabundance with respect to the weaker lines and are more sensitive to the variation of damping constants C_6. Other elements (Gehren et al. 2001, Fe I) also present evidence that Anstee & O'Mara's data may require corrections for particular multiplets.

Alternatively, one may think of possible mineralogical processes that may change the distribution of elements within the CI chondrite parent body, in particular aqueous alteration (Lodders 2003). Our measurements may indicate that the meteoritic CI chondrite abundance requires further investigation.

Finally, if we accept that the NLTE solar photospheric Mn abundance and the meteoritic CI chondrite abundance are correct to within their respective uncertainties, then one may ask: is there a reason why Mn is depleted in the photosphere? There exists a hypothesis that Mn experiences a significant first ionisation potential (FIP) effect, see Feldman & Widing (2002). However, without elaborate investigation this idea remains a speculation. We, of course, encourage future research into the possible influence of FIP effects on the photospheric – meteoritic abundance comparison.

Acknowledgements. M.B. acknowledges with gratitude the Max-Planck Institute for Extraterrestrial Physics (Germany) and IMPRS-Marie Curie Training Site for her Ph.D. fellowship. R.B.W. gratefully acknowledges funding from the Leverhulme Trust and PPARC, UK. R.B.W. would also like to thank and acknowledge G. Nave, National Institute of Standards and Technology, USA, for IR Mn I spectra for the IR branches of the $e^6S_{2.5}$ level.

References

Anstee, S. D., & O'Mara, B. J. 1995, MNRAS, 276, 859
Bergemann, M., & Gehren. T. 2007, A&A, accepted
DOI: 10.1051/0004-6361:20066810 (Paper I)
Blackwell, D. E., & Collins, B. S. 1972, MNRAS, 157, 255
Blackwell-Whitehead, R. J., Pickering, J. C., Pearse, O., & Nave, G. 2005a, ApJS, 157, 402
Blackwell-Whitehead, R. J., Xu, H. L., Pickering, J. C., Nave G., & Lundberg, H. 2005b, MNRAS, 361, 1281
Blackwell-Whitehead, R. J., Lundberg, H., & Nave, G., et al. 2006, MNRAS, 373, 1603
Booth, A. J., Blackwell, D. E., Petford, A. D., & Shallis, M. J. 1984a, MNRAS, 208, 147
Booth, A. J., Blackwell, D. E., & Shallis, M. J. 1984b, MNRAS, 209, 77
Feldman, U., & Widing, K. G. 2002, Phys. Plas., 9, 629
Fuhr, J. R., & Wiese, W. L. 2003, NIST Atomic Transition Probability Tables, in Handbook of Chemistry and Physics, 84th Ed., ed. D. R. Lide (CRC, Boca Raton, FL: Press), 10
Holweger, H., & Müller, E. A. 1974, Sol. Phys., 39, 19
Gehren, T., Butler, K., Mashonkina, L., Reetz, & J., Shi, J. 2001, A&A, 366, 981
Greenlee, T. R., & Whaling, W. 1979, J. Quant. Spectrosc. Radiat. Transfer, 21, 55
Grupp, F. 2004, A&A, 420, 289
Kurucz, R. L., & Bell, B. 1995, Atomic Line Data, Kurucz CD-ROM No. 23. (Cambridge, Mass.: Smithsonian Astrophysical Observatory)
Kurucz, R. L., Furenlid, I., Brault, J., & Testerman, L. 1984, Solar Flux Atlas from 296 to 1300 nm, in Nat. Solar Obs. Atlas, Sunspot, New Mexico
Lodders, K. 2003, ApJ, 591, 1220
Marek, J. 1975, A&A, 44, 69
Norlén, G. 1973, Phys. Scr., 8, 249
Rutten, R. J. 2002, J. Astron. Data, 8, 8
Schnabel, R., Bard, A., & Kock, M. 1995, Z. Phys. D, 34, 223
Steenbock, W., & Holweger, H. 1984, A&A, 130, 319

Online Material

Table 1. New and remeasured laboratory oscillator strengths for Mn I.

Upper level	Lower level	Wavenumber (cm^{-1})	λ_{air} (Å)	*BF*	This Work Log(gf)	*Unc.*(dex)	Previous Work Log(gf)	Ref.[b]	Calc.[a] Log(gf)
$e\ ^8S_{3.5}$	$z\ ^8P_{2.5}$	21 028.888	4754.0338	0.2535	−0.07	0.02	−0.09	3	−0.09
E = 39 431.31 cm^{-1}	$z\ ^8P_{3.5}$	20 899.706	4783.4190	0.3344	0.06	0.02	0.04	3	0.04
τ = 8.07 ± 0.19 ns[c]	$z\ ^8P_{4.5}$	20 726.008	4823.5080	0.4121	0.15	0.02	0.14	3	0.14
Residual				0.0001					
$e\ ^6S_{2.5}$	$z\ ^8P_{3.5}$	22 872.341	4370.8646	0.0003	−3.59	0.08			−3.03
E = 41 403.93 cm^{-1}	$z\ ^6P_{1.5}$	16 624.678	6013.4885	0.2134	−0.43	0.05	−0.25	3	−0.25
τ = 18.5 ± 1.8 ns[d]	$z\ ^6P_{2.5}$	16 615.976	6016.6380	0.3211	−0.25	0.05			−0.22
	$z\ ^6P_{3.5}$	16 601.751	6021.7932	0.4280	−0.12	0.05	0.03	3	0.03
	$y\ ^6P_{1.5}$	5714.003	17 496.0867	0.0089	−0.88	0.05			−0.93
	$y\ ^6P_{2.5}$	5678.129	17 606.6275	0.0123	−0.73	0.05			−0.77
	$y\ ^6P_{3.5}$	5634.016	17 744.4833	0.0156	−0.62	0.05			−0.67
Residual				0.0005					
$z\ ^6D^e_{3.5}$	$a\ ^6S_{2.5}$	41 932.657	2384.0491	0.0008	−3.10	0.08			−2.48
E = 41 932.64 cm^{-1}	$a\ ^6D_{4.5}$	24 880.356	4018.0994	0.2493	−0.19	0.03	−0.31	2	−0.31
τ = 10.87 ± 0.24 ns	$a\ ^6D_{3.5}$	24 650.639	4055.5445	0.4697	−0.59	0.03	−0.07	3	−0.07
	$a\ ^6D_{2.5}$	24 481.126	4083.6266	0.2781	−0.35	0.03	−0.25	3	−0.25
	$a\ ^4D_{3.5}$	18 635.987	5364.4703	0.0021	−2.79	0.04			−2.90
Residual				0.0003					
$z\ ^6D_{0.5}$	$a\ ^6D_{1.5}$	24 630.111	4058.9247	0.7858	−0.46	0.02	−0.45	3	−0.45
E = 42 198.56 cm^{-1}	$a\ ^6D_{0.5}$	24 561.434	4070.2741	0.2097	−1.03	0.02	−0.95	2	−0.95
τ = 11.08 ± 0.31 ns	$a\ ^4D_{0.5}$	18 479.895	5409.7823	0.0043	−2.47	0.02			−3.62
Residual				0.0001					
$z\ ^6F_{3.5}$	$a\ ^6D_{4.5}$	26 471.793	3776.5331	0.0039	−2.41	0.12	−2.51	1	−2.49
E = 43 524.08 cm^{-1}	$a\ ^6D_{3.5}$	26 242.091	3809.5905	0.2491	−0.60	0.02	−0.64	1	−0.60
τ = 17.14 ± 0.35 ns	$a\ ^6D_{2.5}$	26 072.576	3834.3599	0.6847	−0.15	0.02	−0.14	1	−0.12
	$a\ ^4D_{3.5}$	20 227.434	4942.4014	0.0020	−2.46	0.05	−2.82	1	−2.79
	$a\ ^4D_{2.5}$	19 974.872	5004.8938	0.0317	−1.25	0.02	−1.66	1	−1.63
	$a\ ^4G_{4.5}$	18 238.492	5481.3864	0.0278	−1.23	0.02	−1.87	1	−1.87
	$a\ ^4G_{3.5}$	18 236.428	5482.0069	0.0006	−2.92	0.10			−3.44
Residual				0.0002					
$z\ ^4F_{4.5}$	$a\ ^6D_{4.5}$	27 236.449	3670.5053	0.0077	−2.00	0.09	−1.95	1	−1.92
E = 44 288.76 cm^{-1}	$a\ ^6D_{3.5}$	27 006.727	3701.7278	0.0108	−1.85	0.05	−1.78	1	−1.75
τ = 15.69 ± 0.33 ns	$a\ ^4D_{3.5}$	20 992.078	4762.3702	0.9245	0.30	0.02	0.28	1	0.42
	$a\ ^4G_{5.5}$	19 023.064	5255.3139	0.0507	−0.87	0.04	−0.90	1	−0.76
	$a\ ^4G_{4.5}$	19 003.376	5260.7587	0.0039	−1.98	0.02	−2.01	1	−1.97
	$b\ ^4D_{3.5}$	13 934.586	7174.4107	0.0011	−2.29	0.04	−2.44	1	−2.44
	$a\ ^4F_{4.5}$	9350.382	10 691.8212	0.0012	−1.89	0.03			−3.06
Residual				0.0002					
$z\ ^4F_{3.5}$	$a\ ^6D_{3.5}$	27 241.454	3669.8308	0.0062	−2.20	0.04	−2.01	1	−1.99
E = 44 523.45 cm^{-1}	$a\ ^6D_{2.5}$	27 071.942	3692.8103	0.0061	−2.20	0.03	−2.14	1	−2.12
τ = 15.70 ± 0.41 ns	$a\ ^4D_{3.5}$	21 226.794	4709.7092	0.1911	−0.49	0.02	−0.49	1	−0.34
	$a\ ^4D_{2.5}$	20 974.239	4766.4207	0.7355	0.11	0.02	0.08	1	0.10
	$a\ ^4G_{4.5}$	19 238.094	5196.5730	0.0513	−0.98	0.02	−0.96	1	−0.93
	$a\ ^4G_{3.5}$	19 235.792	5197.1950	0.0069	−1.85	0.02	−1.83	1	−1.81
	$b\ ^4D_{3.5}$	14 169.281	7055.5755	0.0008	−2.52	0.03	−2.56	1	−2.56
	$b\ ^4D_{2.5}$	14 103.873	7088.2968	0.0003	−2.93	0.05			−2.89
Residual				0.0019					
$z\ ^4F_{2.5}$	$a\ ^6D_{2.5}$	27 244.729	3669.3897	0.0038	−2.53	0.05	−2.41	1	−2.41
E = 44 696.29 cm^{-1}	$a\ ^6D_{1.5}$	27 127.791	3685.2076	0.0028	−2.67	0.05	−2.62	1	−2.59
τ = 15.58 ± 0.37 ns	$a\ ^4D_{3.5}$	21 399.582	4671.6807	0.0173	−1.66	0.02	−1.70	1	−1.67
	$a\ ^4D_{2.5}$	21 147.022	4727.4757	0.2793	−0.44	0.02	−0.50	1	−0.47
	$a\ ^4D_{1.5}$	20 976.711	4765.8589	0.6308	−0.08	0.02	−0.10	1	−0.08
	$a\ ^4G_{2.5}$	19 415.276	5149.1490	0.0074	−1.95	0.02	−1.92	1	−1.90
	$a\ ^4G_{3.5}$	19 408.577	5150.9262	0.0558	−1.07	0.02	−1.05	1	−1.03

Table 1. continued.

Upper level	Lower level	Wavenumber (cm^{-1})	λ_{air} (Å)	*BF*	This Work Log (gf)	*Unc.*(dex)	Previous Work Log (gf)	Ref.[b]	Calc.[a] Log (gf)
	$b\ ^4D_{2.5}$	14 276.656	7002.5103	0.0009	−2.62	0.04			−2.61
	$b\ ^4D_{1.5}$	14 270.557	7005.5028	0.0004	−2.98	0.06			−3.06
	$a\ ^4F_{2.5}$	9581.236	10 434.2077	0.0002	−2.94	0.07			−3.09
	$a\ ^4F_{1.5}$	9531.636	10 488.5040	0.0002	−2.95	0.07			−4.13
Residual				0.0014					
$z\ ^4F_{1.5}$	$a\ ^4D_{2.5}$	21 265.444	4701.1493	0.0291	−1.60	0.03	−1.66	1	−1.65
E = 44 814.73 cm^{-1}	$a\ ^4D_{1.5}$	21 095.139	4739.1031	0.2894	−0.60	0.02	−0.66	1	−0.49
τ = 15.43 ± 0.56 ns	$a\ ^4D_{0.5}$	20 995.814	4761.5226	0.6144	−0.27	0.02	−0.30	1	−0.14
	$a\ ^4G_{2.5}$	19 533.707	5117.9299	0.0614	−1.20	0.02	−1.16	1	−1.14
Residual				0.0058					
$z\ ^4D_{3.5}$	$a\ ^4D_{3.5}$	22 457.627	4451.5807	0.7382	0.13	0.02	0.14	1	0.28
E = 45 754.27 cm^{-1}	$a\ ^4D_{2.5}$	22 205.072	4502.2127	0.1955	−0.43	0.02	−0.50	1	−0.34
τ = 12.94 ± 0.30 ns	$a\ ^4P_{2.5}$	18 552.871	5388.5030	0.0088	−1.62	0.02	−1.70	1	−1.69
	$b\ ^4D_{3.5}$	15 400.103	6491.6693	0.0348	−0.87	0.02	−1.07	1	−1.04
	$b\ ^4D_{2.5}$	15 334.704	6519.3550	0.0045	−1.75	0.02	−1.24	1	−1.25
	$b\ ^4P_{2.5}$	11 928.849	8380.7351	0.0039	−1.60	0.03	−1.79	1	−1.79
	$a\ ^4F_{4.5}$	10 815.702	9243.2802	0.0080	−1.20	0.02	−1.35	1	−1.35
	$a\ ^4F_{3.5}$	10 712.988	9331.9035	0.0010	−2.10	0.05			−2.14
Residual				0.0053					
$z\ ^4D_{2.5}$	$a\ ^4D_{3.5}$	22 644.331	4414.8765	0.2803	−0.41	0.02	−0.40	1	−0.29
E = 45 940.93 cm^{-1}	$a\ ^4D_{2.5}$	22 391.775	4464.6725	0.4126	−0.24	0.02	−0.25	1	−0.10
τ = 12.72 ± 0.29 ns	$a\ ^4D_{1.5}$	22 221.464	4498.8915	0.2436	−0.46	0.02	−0.49	1	−0.34
	$a\ ^4P_{2.5}$	18 739.578	5334.8154	0.0008	−2.78	0.03	−2.88	1	−2.86
	$a\ ^4P_{1.5}$	18 693.192	5348.0537	0.0087	−1.75	0.02	−1.81	1	−1.78
	$b\ ^4D_{3.5}$	15 586.760	6413.9286	0.0073	−1.67	0.02	−1.94	1	−1.91
	$b\ ^4D_{2.5}$	15 521.408	6440.9342	0.0238	−1.16	0.02	−1.42	1	−1.42
	$b\ ^4D_{1.5}$	15 515.308	6443.4665	0.0083	−1.61	0.02	−1.79	1	−1.76
	$b\ ^4P_{2.5}$	12 115.626	8251.5353	0.0011	−2.28	0.15			−2.39
	$b\ ^4P_{1.5}$	11 477.680	8710.1701	0.0020	−1.97	0.04			−1.91
	$a\ ^4F_{3.5}$	10 899.682	9172.0627	0.0067	−1.40	0.02	−1.50	1	−1.50
	$a\ ^4F_{2.5}$	10 826.100	9234.4029	0.0014	−2.07	0.04			−2.03
Residual				0.0032					
$z\ ^4D_{1.5}$	$a\ ^4D_{2.5}$	22 534.739	4436.3474	0.4054	−0.43	0.02	−0.43	1	−0.29
E = 46 083.89 cm^{-1}	$a\ ^4D_{1.5}$	22 364.429	4470.1318	0.2901	−0.56	0.02	−0.57	1	−0.44
τ = 12.76 ± 0.42 ns	$a\ ^4D_{0.5}$	22 265.104	4490.0734	0.2472	−0.63	0.02	−0.64	1	−0.52
	$a\ ^4P_{2.5}$	18 882.539	5294.4249	0.0009	−2.94	0.04			−3.01
	$a\ ^4P_{0.5}$	18 802.114	5317.0717	0.0047	−2.20	0.02	−2.26	1	−2.23
	$b\ ^4D_{0.5}$	15 672.302	6378.9202	0.0098	−1.72	0.02	−1.83	1	−1.83
	$b\ ^4D_{2.5}$	15 664.371	6382.1497	0.0112	−1.67	0.02	−1.58	1	−1.80
	$b\ ^4D_{1.5}$	15 658.272	6384.6356	0.0181	−1.46	0.02	−1.86	1	−1.53
	$b\ ^4P_{1.5}$	11 620.623	8603.0275	0.0015	−2.29	0.07			−2.27
	$b\ ^4P_{0.5}$	11 238.669	8895.4084	0.0011	−2.39	0.05			−2.32
	$a\ ^4F_{2.5}$	10 969.070	9114.0416	0.0068	−1.57	0.02	−1.80	1	−1.80
	$a\ ^4F_{1.5}$	10 918.990	9155.8436	0.0018	−2.16	0.03			−2.14
Residual				0.0014					
$z\ ^4D_{0.5}$	$a\ ^4D_{1.5}$	22 450.473	4452.9992	0.5126	−0.62	0.02	−0.62	1	−0.49
E = 46 169.93 cm^{-1}	$a\ ^4D_{0.5}$	22 351.149	4472.7878	0.4302	−0.69	0.02	−0.72	1	−0.58
τ = 12.75 ± 0.34 ns	$a\ ^4P_{0.5}$	18 888.152	5292.8513	0.0017	−2.94	0.06	−2.94	1	−2.90
	$b\ ^4D_{0.5}$	15 758.347	6344.0891	0.0217	−1.69	0.02	−1.86	1	−1.80
	$b\ ^4D_{1.5}$	15 744.317	6349.7425	0.0182	−1.76	0.02	−1.85	1	−1.84
	$b\ ^4P_{0.5}$	11 324.749	8827.7937	0.0031	−2.24	0.08			−2.36
	$a\ ^4F_{1.5}$	11 004.978	9084.3037	0.0086	−1.78	0.02	−2.02	1	−2.02
Residual				0.0039					

[a] The semi-empirical calculations are taken from Kurucz & Bell (1995).
[b] The previous laboratory values are taken from (1) Greenlee & Whaling (1979); (2) Blackwell & Collins (1972); and (3) Booth et al. (1984a).
[c] The level lifetimes are taken from Schnabel et al. (1995) unless stated otherwise.
[d] Lifetime for the level $e\ ^6S_{2.5}$ is taken from Marek (1975).
[e] Branching fractions and oscillator strengths for $z\ ^6D_{3.5}$ are taken from Blackwell-Whitehead et al. (2005b).